PHYSICAL REVIEW D VOLUME 40, NUMBER 5 1 SEPTEMBER 1989

Hadron properties in lattice QCD with dynamical fermions

K. D. Born
Institut für Theoretische Physik, Rheinisch-Westfälische Technische Hochschule Aachen, D-5100 Aachen, Federal Republic of Germany

E. Laermann
Fachbereich Physik, Bergische Universität, D-5600 Wuppertal, Federal Republic of Germany

N. Pirch
Institut für Theoretische Physik, Rheinisch-Westfälische Technische Hochschule Aachen, D-5100 Aachen, Federal Republic of Germany

T. F. Walsh
Physics Department, University of Minnesota, Minneapolis, Minnesota 55455

P. M. Zerwas
Institut für Theoretische Physik, Rheinisch-Westfälische Technische Hochschule Aachen, D-5100 Aachen, Federal Republic of Germany
(Received 17 January 1989)

Incorporating dynamical Kogut-Susskind fermions into a Monte Carlo simulation of QCD, we have analyzed the masses of low-lying hadrons, chiral-symmetry breaking, and the interquark potential. We used a 24×12^3 lattice for two couplings g, where $\beta=6/g^2=5.20$ and 5.35. The quark masses were $ma=0.075$, 0.050, and 0.025 (a being the lattice spacing). We find that the pattern of hadron masses of the π, ρ, and N is qualitatively as seen experimentally. The pion mass squared is proportional to the quark mass and thus behaves as expected from chiral symmetry. Values for the quark condensate extrapolated to $ma=0$, the renormalization-group-invariant quark mass, and the pion decay constant are in reasonable agreement with values derived from experiment or from current algebra. If we fix the lattice spacing from the ρ mass, we see evidence for the screening effect of light-quark–antiquark pairs in the potential between two massive quarks. At $\beta=5.20$ and $ma=0.050$ we find good agreement between the results from our pseudofermion method and those from a hybrid simulation.

I. INTRODUCTION

Numerical simulations of quantum chromodynamics have achieved several semiquantitative successes—for example, a reasonable spectrum of low-lying hadrons, spontaneous chiral-symmetry breaking (implying the existence of an almost massless pion) and a rising potential between heavy quarks. These calculations were based on integration of QCD over space-time lattices, mostly without including the effect of the creation and annihilation of virtual quark-antiquark pairs (the "valence quark" or "quenched" approximation). It is a reasonable first step towards a more exact treatment to ask whether or not the inclusion of virtual quark pairs or dynamical fermions dramatically changes these known quenched approximation results. It is also important to demonstrate that different technical approaches to exact QCD can produce comparable results. While only a few attempts in this direction have been reported, the field is expanding rapidly.[1]

In this paper we report on our investigation of the low-lying meson and baryon masses, the quark condensate in the QCD vacuum, and the potential between heavy quarks. We thereby extend previous work on this problem in two-color SU(2) (Ref. 2), which anticipated many of the patterns now observed in the technically more demanding three-color SU(3) with dynamical fermions.

Our calculation is carried out on a 24×12^3 lattice and includes four degenerate Kogut-Susskind fermions. The fermionic degrees of freedom are incorporated using the pseudofermion technique.[3]

We have taken data at two values of the coupling, $6/g^2=\beta=5.20$ and 5.35, and three quark mass values $ma=0.075$, 0.050, and 0.025, where a is the lattice spacing. We expect to approach approximate asymptotic scaling in this β range and yet stay below the deconfinement phase transition for the above lattice size.[4,5]

For these parameters, our lattice spacing is ~0.2 fm and the entire spatial lattice volume is roughly $(2.4\text{ fm})^3$. This provides a reasonable number of computational points and links inside a hadron of approximately 1-fm diameter, together with a spatial box about twice the expected proton size. We estimate that this situation would correspond to a physical quark mass parameter $ma\sim0.005$, requiring an extrapolation from our present measured values before contact with experiment can be made. Nevertheless, the results obtained down to $ma=0.025$ are quite encouraging on several points.

The systematic errors inherent in any computer experiment can be controlled by comparing the results with

 ©1989 The American Physical Society

those that have been obtained by very different numerical methods. Luckily enough, an independent analysis based on a hybrid method has been carried out at $\beta=5.20$, $ma=0.050$ in the confinement region on a $(2\cdot16)\times8^3$ lattice.[5] The agreement is very satisfactory, providing a mutual cross-check of different systematic errors.

The paper is organized as follows. After a short description of the method and the technique we used, we present the results on the low-lying hadron masses, the chiral sector, and the interquark potential.

II. COMPUTATIONAL METHOD

Including four degenerate Kogut-Susskind quarks with mass m, the pure gauge action is supplemented by the logarithm of the Dirac determinant,

$$S_{\text{eff}}=\beta\sum_{\square}[1-\tfrac{1}{6}\operatorname{tr}(U_{\square}+U_{\square}^{\dagger})]-\operatorname{tr}\ln[D(U)+ma] \tag{1}$$

once the quark fields are integrated out. In this expression,

$$[D(U)+ma]_{m,n}=\tfrac{1}{2}\sum_{\mu}\Gamma_{\mu}(m)[U_{\mu}(m)\delta_{m+\mu,n}-U_{\mu}^{\dagger}(n)\delta_{m-\mu,n}]+ma\delta_{m,n}\ . \tag{2}$$

The sum in (1) runs over the (ordered) plaquettes $U_{\square}$; $U_{\mu}(n)$ denote the link variables and $\Gamma_{\mu}(m)=(-)^{m_1+m_2+\cdots+m_{\mu-1}}$.

To generate the equilibrium gauge-field configurations we used the Metropolis algorithm. If we allow only a small variation δU in the tentative upgrade $U\to U+\delta U$, then the change in the fermionic part of the action can be linearized,

$$\delta S_F=-\operatorname{Re}\operatorname{tr}J_{\mu}(n)\delta U_{\mu}(n)+O([\delta U]^2)\ , \tag{3}$$

and $\delta U_{\mu}(n)$ interacts only locally with the current:

$$J_{\mu}(n)=\tfrac{1}{2}\Gamma_{\mu}(n)\{[D(U)+ma]^{-1}-\text{H.c.}\}_{n+\mu,n}\ . \tag{4}$$

For small $\delta U_{\mu}(n)$, all the required elements of the propagator $[D(U)+ma]^{-1}$ can be computed before performing the link upgrade. This leaves us with an error of order $[\delta U]^2$, consistent with the linearization of δS_F. We calculate the propagators using the pseudofermion method. Since the propagator is not a positive-definite matrix, we generate complex boson fields $\phi(n)$ with a distribution having weight

$$\exp(-S_{\text{PF}})=\exp[-\phi^{\dagger}(D^{\dagger}+ma)(D+ma)\phi]\ . \tag{5}$$

The fermion propagator is then given in terms of the correlation function of the complex boson fields:

$$[D(U)+ma]^{-1}_{n+\mu,n}=\sum_{k}\langle\phi_{n+\mu}\phi_{k}^{*}\rangle(D^{\dagger}+ma)_{k,n}\ . \tag{6}$$

It is most efficient to update the boson fields ϕ by means of the heat-bath algorithm.[6]

Except for the first runs, in which we thermalized pure gauge systems, we begin each run with a configuration that is equilibrated at the previous quark mass value. After updating all gauge links once, the pseudofermions are allowed to adjust to the gauge-field configuration for 75–100 sweeps. Following this, 50–100 pseudofermion sweeps are used to measure the currents $J_{\mu}(n)$. The entire process is then repeated, starting with a new gauge-field update. Every sweep we generate a new table of 800 SU(3) matrices ΔU, plus their Hermitian conjugates, via $\Delta U=\exp(i\alpha^a\lambda^a)$, where the λ's represent the eight Gell-Mann matrices. The U's are kept close to the unit matrix by taking each α^a from a Gaussian distribution which is cut between 0.075 to 0.04, and varying the cut over the quark mass and β range that we investigated. The exponential is expanded to the fourth power and then reunitarized. Constructing $U^{\text{new}}=U^{\text{old}}\times\Delta U$ with ΔU chosen randomly from the 1600 entries in the table, we settle at gauge-field acceptance rates between 85% and 92%. On the other hand, we have checked that we traverse the group space approximately within 300 steps for a single isolated link variable. With this choice it still requires 4000–5000 gauge field sweeps to reach equilibrium for the combined gauge and pseudofermion field system. Experimentation within the limits set by our computer resources has shown us that the chosen acceptance rates and pseudofermion updates lead to measured quantities which do not exhibit marked changes when further increasing either the number of pseudofermion sweeps per gauge field sweep or the gauge-field acceptance rate. It is for this reason that we vary these quantities slightly with quark mass and β. We continuously monitor the time development of the plaquette and other observables. After this long equilibration of the combined system of gauge and pseudofermion fields, we took data for an additional 5000–8000 gauge-field sweeps for each value of the coupling and each of the three quark masses; see Table I. Data were recorded every 50th gauge field sweep of the lattice. We thus record typically 100–150 configurations at each pair of β, m values.

Computer experiments, not unlike real experiments, have unavoidable statistical and systematic errors which have to be investigated. The pseudofermion method can in principle be made arbitrarily accurate, given enough computer time. However, practical application of it—as of any of the known algorithms including exact ones—necessarily involves compromises. The linearization in δU may systematically underestimate the influence of virtual quarks as a consequence of Jensen's inequality (slightly shifting the β value). The pseudofermion fields can be subject to statistical biases when the number of updates is small. The effect of these errors on the numer-

TABLE I. The number of thermalization plus measurement sweeps at the β and m values investigated in this experiment.

β \ m	0.075	0.050	0.025
5.20	5000 +3000	2500 +3000	5000 +7000
5.35	5000 +4000	4000 +4000	5000 +5000

ical results is not known *a priori* but has to be studied with care.[7]

During the measurements we found sweep-to-sweep correlations over several hundred sweeps. They increase with decreasing quark masses. But we did not observe any long-term drifts, either in local observables such as the plaquette and vacuum condensate or in the particle propagation over long distances. The stability is demonstrated in Figs. 1(a) and 1(b) and Figs. 2(a) and 2(b) for the most critical quark mass value 0.025. This is in contrast with Ref. 8, where the algorithmic and physical parameters were substantially different from ours. The analysis there has been carried out with three fermionic degrees of freedom on a 32×10^3 lattice at a high β value of 5.70. The pseudofermionic current has been averaged over 25 measurements (compared to 50–100 here). The gauge fields were updated with eight Metropolis hits per link at an acceptance rate of 81% (90% at $ma=0.02$). First, if the multihit approach is to be of practical use, this must translate into a one-hit acceptance rate lower than our 85–92 %, corresponding to larger δU's. Second, only 1000 randomly chosen sites out of 32 000 were updated between each of 300 pseudofermion sweeps carried out before a gauge-field sweep. According to our experiment this is not sufficient to let the (pseudo)fermions follow the time development of the gauge fields properly.

Another point of interest is that the data of Ref. 8 seem to indicate a restoration of chiral symmetry, at least for $ma=0.02$; this does not seem implausible at β as high as 5.7 (see also Ref. 1). Based on the experience gathered in unquenched finite temperature analyses for four dynamical Kogut-Susskind fermions,[4,5] we estimate the deconfinement transition to be located at $\beta=5.35$ for a lattice time extension $N_T=12$ at $ma=0$. The slope of β_c vs ma does not appear to depend much on N_T for $N_T\geq8$. In order to be sure that we are not affected by finite-temperature effects, we checked the values of the Polyakov loops, in addition to the chiral condensate, at our most critical values of the parameters, $\beta=5.35$ and $ma=0.025$, Fig. 3. We see no evidence for an onset of deconfinement.

III. HADRON MASSES

In the Kogut-Susskind version of the fermion theory, quark fields are smeared out over the unit cells of the lat-

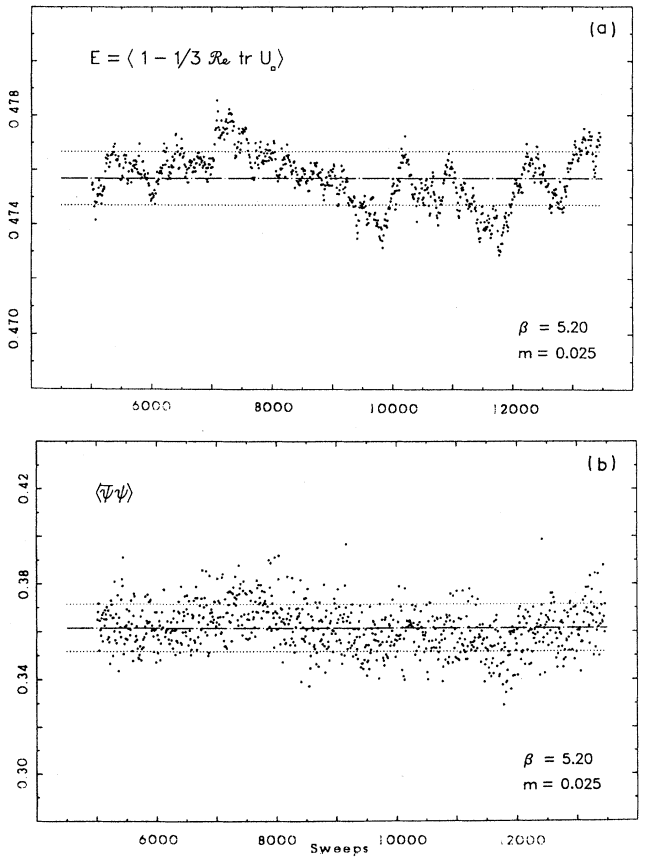

FIG. 1. Time evolution of the plaquette (a) and the chiral condensate (b) at $\beta=5.20$ for the quark mass $ma=0.025$. The dotted lines represent the mean value and the upper (lower) bound on the mean error of a single measurement. 8000 sweeps are plotted after 5000 thermalization sweeps.

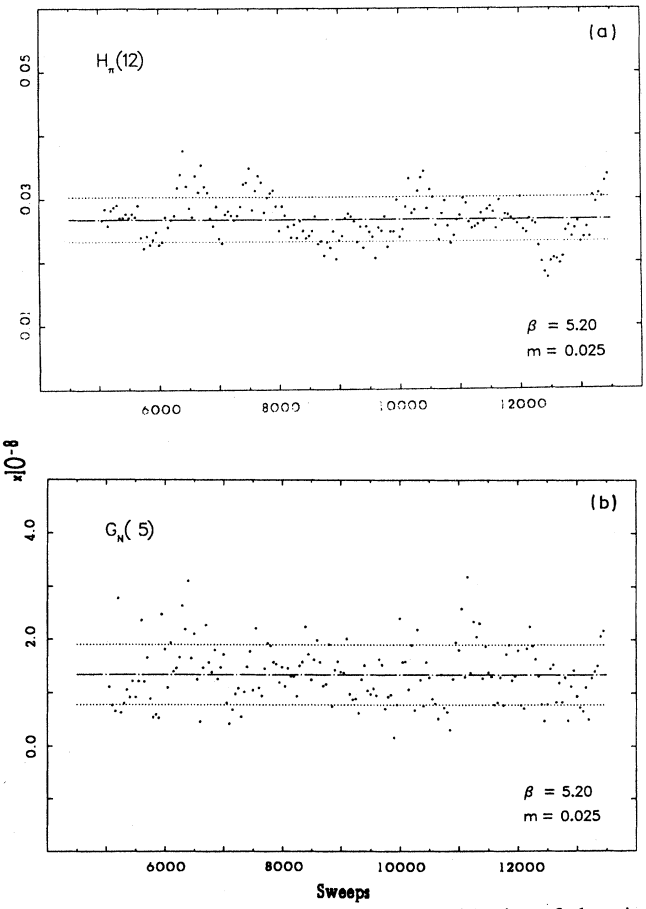

FIG. 2. (a) The time evolution of the midpoint of the pion propagator at $\beta=5.20$ and $ma=0.025$. Dotted lines and statistics as in Fig. 1. (b) The same for the nucleon propagator at $t=5$.

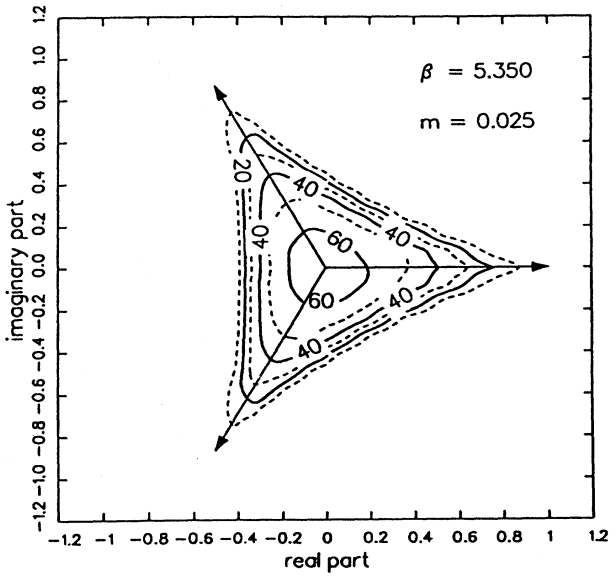

FIG. 3. Distribution of the Polyakov loops in the complex plane for the most critical parameter set $[\beta,ma]=[5.35,0.025]$. Note that the plot closely resembles the distribution in the confined phase of the quenched analysis (Ref. 9)—differing strongly from the deconfined phase.

tice with sites occupied by one-component staggered fields χ. Local meson and baryon operators with the appropriate continuum quantum numbers are constructed from the quark fields in the standard way.[10] The propagators of those fields which determine the hadron masses can be expressed in terms of suitable linear combinations of correlation functions of the χ fields.

Mesons

The propagators are given in terms of the meson masses by

$$\sum_{\mathbf{n}} \sigma(\mathbf{n})\langle |G(\mathbf{n},t)|^2\rangle = Ae^{-mt}+(-)^t A'e^{-m't}+\cdots , \quad (7)$$

where $\sigma(\mathbf{n})$ collects the right combinations of quark propagators $G(\mathbf{n},t)$ to project out the appropriate continuum states, Table II.

There are opposite parity states in (7) that oscillate in discrete time t, a feature of the Kogut-Susskind formulation of lattice fermions. Possible additional contributions from higher-mass states are indicated by ellipsis. In order to include the effect of a lattice periodic in the time direction we have simply to replace $e^{-mt}\to e^{-mt}+e^{-m(T-t)}$, where T is the temporal extent of the lattice.

TABLE II. Phase factors projecting the appropriate spin-parity quantum numbers out of the correlation functions.

$\sigma(\mathbf{n})$	Particles
1	$\pi+?$
$(-1)^{n_1+n_2+n_3}$	$\pi'+\epsilon$
$(-1)^{n_1}+(-1)^{n_2}+(-1)^{n_3}$	$\rho+B$
$(-1)^{n_1+n_2}+(-1)^{n_2+n_3}+(-1)^{n_1+n_3}$	$\rho'+A_1$

Baryons

Here we have

$$\sum_{\mathbf{n}\ \text{even}} \langle G(\mathbf{n},t)G(\mathbf{n},t)G(\mathbf{n},t)\rangle_{\mathrm{AS}} = Ae^{-mt}+(-)^t A'e^{-m't}+\cdots , \quad (8)$$

where the color indices are antisymmetrized and m, m' correspond to the masses of the even-parity proton and a state of opposite parity. Periodicity requires the substitution $e^{-mt}\to e^{-mt}+(-)^t e^{-m(T-t)}$.

We calculated the propagators by the conjugate-gradient method. The iterations were stopped when the total length of the rest vector fell below 10^{-4}–10^{-5}. The smaller value was chosen for smaller quark masses. For these numbers the relation $(D+ma)_{lm}(D+ma)^{-1}_{mn}=\delta_{ln}$ was numerically satisfied within six to seven digits, and we did not observe any modification in the propagators when the stopping condition was tightened further. The number of conjugate-gradient iterations necessary to reach this accuracy was between 120 and 400, depending on the quark mass. For each $[\beta,m]$ pair we analyzed 50–170 configurations separated by 50–100 gauge sweeps. Within each configuration eight propagator source points were selected, evaluated for each of the three colors. As a typical example, we display the time dependence of the π,ρ,N propagators for $\beta=5.35$ and $ma=0.050$ in Fig. 4. The influence of the parity partners is indicated by the double lines. The error bars shown follow from a simple

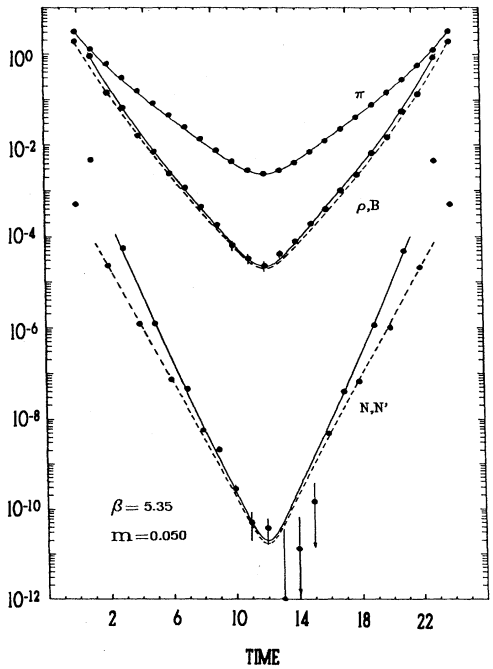

FIG. 4. The time development of the π,ρ,N propagators for $\beta=5.35$ and $ma=0.050$. The influence of the parity partners B to ρ and N' to N is indicated by the double lines.

statistical analysis. However, chopping the data into blocks of 1–12 measurements and treating each block as one independent entry in the statistics program did not change the errors significantly.

It is important to realize that our data for low t and for t near T are independent. In fact, fits separately to the small-t and large-t data provide us a check on possible systematic errors.

The mean values of the hadron masses are based on symmetric fits to the propagators over the range from $t_{\min}$ to $T-t_{\min}$, where $t_{\min}$ as well as the number of contributing particles were varied. The generally adopted fitting procedure started with single-particle fits over the entire t range, followed by successive increases of $t_{\min}$. The mass estimates must become independent of $t_{\min}$ once a high enough value has been reached so that short-time contributions from heavier particles have died out. Consequently, the difference between the plateau value and the results from fits with lower $t_{\min}$ were attributed to the presence of opposite-parity states and/or higher recurrences. These contributions were then evaluated by including additional states in the fit ansatz. First we try to isolate the opposite-parity partner. Starting with $t_{\min}=1$ we followed the behavior of the masses as $t_{\min}$ was raised until the previously obtained lowest-mass value was reproduced and the value for the new state appeared stable. The narrowing of the fitted t interval was stopped when only the lowest state effectively contributed to the propagator. When we had succeeded in establishing the mass of an opposite-parity state we started the whole procedure again in order to separate higher recurrences of both states. In fact, we will quote the mass of an opposite-parity particle only if we were able to reproduce both masses in a three-state-fit ansatz. We document this procedure in Fig. 5, for a few examples, at $\beta=5.35$ and $ma=0.075$. We show the resuts for the ρ and N. The results of one-, two-, and three-state fits converge very well, leading to excellent mass measurements.

In Table III we present the results of this procedure. The mean values result from fits which show supposedly asymptotic behavior (in the sense discussed above) together with a good χ^2 value. The quoted statistical errors (upper line) are taken from the same MINUIT run. The error in the lower line, which we cautiously call "systematic," is a measure of the variance of fit results over the highest possible $t_{\min}$ values. In addition we analyzed correlation functions for mesons which are defined on even time distances only. Of course, the raw data is the same as before, but the suppression of the parity partner $\propto \tanh(m'a/2)$ can help to disentangle both states. The admixture of the parity partner is going to zero in the continuum limit, but the suppression is not always strong in our simulation since the lattice spacing is not very small. The masses these fits return are in the case of strong mixing most reliable for the lower mass state and for weak mixing for the dominant one. Again, using $t_{\min}$ values as high as possible, we account for this additional information in the estimate of the systematic errors. As a further check on our error analysis, we applied the jackknife method to several of our propagator data sets. The resulting statistical error was very close to the MINUIT error and only a bit larger than this error value for big data-block sizes. We are thus safe in quoting the MINUIT error as our statistical error on the masses. The difference between the two methods of obtaining statistical errors is significantly smaller than the systematic error which we estimated by varying the $t_{\min}$ values and the number of states in the fits.

Some specific channels are noteworthy. No exotic 0^{+-} parity partner is visible in the pion propagator. The ρ/B channel is dominated by the ρ. Even though an oscillating behavior due to a B contribution is visible, an accurate determination of the B mass is difficult. Inspecting the t-even B propagator, we still find a dominant ρ signal. In the ρ'/A_1 correlation function the A_1 admixture is considerably larger allowing the separation of both states through their different oscillatory behavior. Fitting the t-even A_1 propagator we face the problem that for large distances the lighter ρ' is not sufficiently suppressed while for small t we cannot be sure that higher mass contributions have died out. In the π'/ε channel both states contribute with roughly the same strength. The π' can be

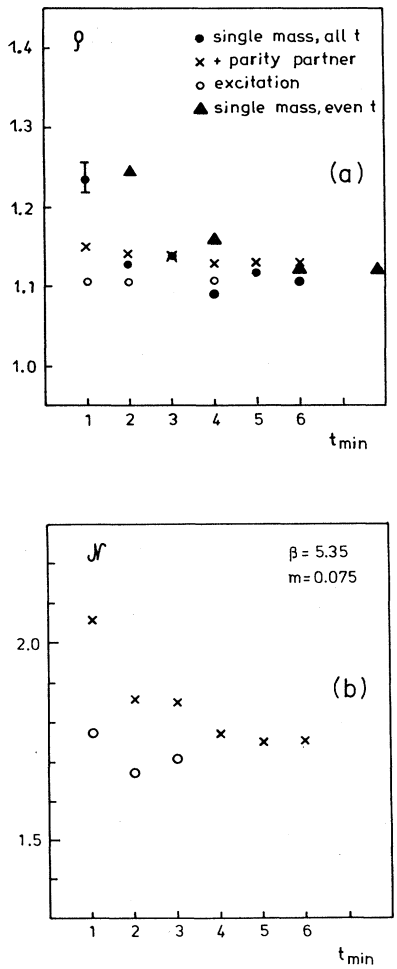

FIG. 5. The fit procedure demonstrated for the ρ and N at $[\beta,ma]=[5.35,0.075]$, see text.

obtained from large t_{min} single-state fits. The ϵ mass is determined from connected Green's functions only (see Ref. 11 for more details). For some of the $[\beta,m]$ values investigated the nucleon propagator submerges in the noise at large t.

At our quark mass values, none of the mesons is significantly unstable to decay. As an example, the ρ meson is still slightly below or close to twice the π mass.

In the following paragraphs we shall evaluate the results of our experiment, collected in Table III.

(i) In Figs. 6 we display our π,ρ,N masses versus the quark masses at both β values. If we choose to make a linear fit to the quark mass dependence of the ρ propagator, then we find the values of Table IV for the ρ mass in the limit of vanishing quark mass. [We have related the lattice mass m_ρ to the continuum mass M_ρ by $aM_\rho/2=\sinh(am_\rho/2)$.] Using the continuum value $M_\rho=770$ MeV we obtain the lattice spacings a in physical units as given in Table IV. Comparing the values at $\beta=5.20$ with $\beta=5.35$, the ratio of the lattice spacings is 1.38 ± 0.08 compared to 1.25 for asymptotic scaling (see also Fig. 7). In the light of these parameters a comparison with experimental numbers is not necessarily futile. Taking the lattice spacings at face value and turning them into $\Lambda_{\overline{MS}}$ values[12] ($\overline{MS}$ denotes the modified

TABLE III. Results of the hadron mass fits in units of the (inverse) lattice spacings for our set of $[\beta,m]$ values.

	$ma=0.025$	$ma=0.050$	$ma=0.075$
		$\beta=5.20$	
π	0.435±0.004	0.620±0.004	0.725±0.024
ρ	1.04 ±0.03	1.12 ±0.02	1.24 ±0.02 ±0.05
N	1.58 ±0.04	1.76 ±0.02 ±0.15	1.90 ±0.02 ±0.10
A_1	1.40 ±0.07	1.45 ±0.03 ±0.05	1.54 ±0.02 ±0.07
$[B]$	1.16 ±0.09	1.33 ±0.04 ±0.06	1.40 ±0.03 ±0.10
ϵ	0.91 ±0.02	1.06 ±0.01 ±0.02	1.22 ±0.02 ±0.02
π'	0.86 ±0.06	1.00 ±0.03 ±0.10	1.13 ±0.17
ρ'	1.14 ±0.06	1.30 ±0.06 ±0.06	1.40 ±0.05 ±0.03
N'	1.74 ±0.08	2.09 ±0.03 ±0.11	2.34 ±0.06 ±0.10
		$\beta=5.35$	
π	0.438±0.003	0.600±0.002	0.725±0.025
ρ	0.83 ±0.02 ±0.05	0.97 ±0.06 ±0.05	1.12 ±0.02 ±0.02
N	1.36 ±0.01 ±0.08	1.60 ±0.01 ±0.08	1.73 ±0.02 ±0.08
A_1	1.13 ±0.02	1.24 ±0.03 ±0.05	1.40 ±0.02 ±0.05
$[B]$	1.02 ±0.03	1.10 ±0.10 ±0.10	1.30 ±0.02 ±0.10
ϵ	0.79 ±0.01	0.94 ±0.01 ±0.01	1.10 ±0.01 ±0.02
π'	0.68 ±0.04	0.80 ±0.10 ±0.10	0.95 ±0.07 ±0.05
ρ'	0.86 ±0.02	0.97 ±0.03 ±0.05	1.16 ±0.05 ±0.06
N'	1.51 ±0.02 ±0.10	1.95 ±0.01 ±0.10	2.10 ±0.05 ±0.10

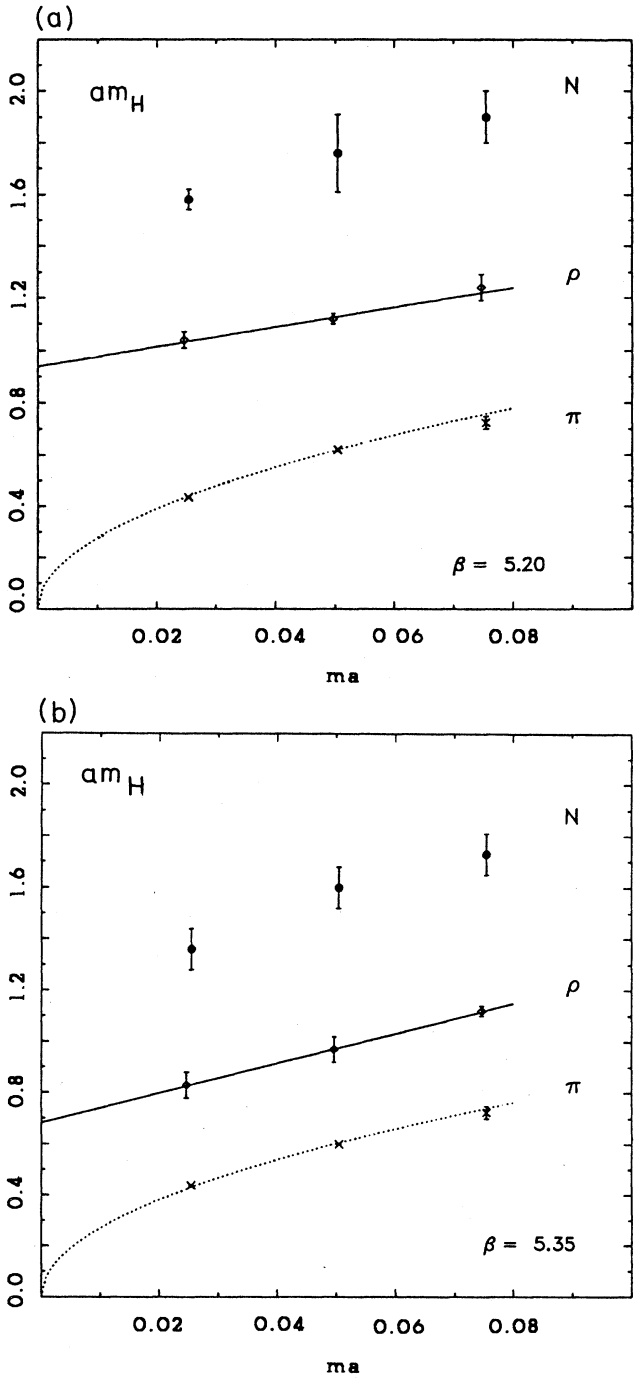

FIG. 6. The spectrum of mesons and the nucleon for three quark mass values at (a) $\beta=5.20$ and (b) $\beta=5.35$. The extrapolation of the ρ mass down to zero quark mass is shown by the solid curve. The π meson data are fitted to the square root of the quark mass.

TABLE IV. ρ masses, corrected for lattice artifacts, in the limit of vanishing quark masses and the lattice spacings a calculated from the physical ρ mass value.

β	$m_\rho a$	a (fm)
5.20	0.960±0.028	0.25±0.01
5.35	0.695±0.035	0.18±0.01

minimal subtraction scheme) by means of the asymptotic scaling formula, we get 60–70 MeV (see also Ref. 1). These values, including those from quenched calculations, are considerably smaller than most of the fits in high-energy scale-breaking analyses.[13,14]

In our view, the appropriate way to make contact with continuum physics is by using the ρ mass to set the lattice spacing. In this way, we expect to minimize the effect of any small ($\sim 10\%$) violation of scaling in our data. We follow this procedure in what follows.

(ii) We find that the general pattern of mass ratios coincides roughly with that obtained from quenched calculations and, more importantly, with the values observed experimentally. Of course, our input parameters lead to a π-to-ρ mass ratio above the experimental value, and similarly for the proton-to-ρ mass ratio. Our results are compared to a compilation[1] of other unquenched calculations in an "Edinburgh plot," Fig. 8. The consistency of the various results is significant because they were obtained by very different computational methods.

(iii) Flavor symmetry is restored in the ρ sector to better than $\sim 5\%$. In the π sector the discrepancy is still large but an improvement is indicated at small quark masses. The situation here appears somewhat worse than in quenched simulations at comparable β values. This seems to be a common feature of mass calculations including dynamical fermions as noted also in Ref. 18.

(iv) We have one set of parameters $\beta = 5.20$ and $ma = 0.050$, which permits us to make numerical comparisons with Ref. 5 at the same values in the confinement region. Those simulations were carried out by means of a hybrid method on a 16×8^3 lattice, doubled in the time direction for calculating the hadron propagators. When we compare the results for the hadron masses (Table V), we find very satisfactory agreement, especially in view of the fact that the two methods are rather different and are subject to systematic errors of different origin. Because the lattice sizes are different in the two calculations we conclude that finite-size effects do not disrupt our analysis. This observation is corroborated in a companion paper on two-color SU(2) (Ref. 11).

IV. CHIRAL-SYMMETRY BREAKING

The Kogut-Susskind action is invariant under a continuous flavor nonsinglet chiral transformation. Consequently, we can examine whether or not the lattice undergoes a spontaneous breakdown of chiral symmetry. This is signaled by a finite value of the vacuum quark condensate in the zero-quark-mass limit, associated with the existence of a zero-mass Goldstone particle, the pion.

Within errors, we find that the pion mass squared is

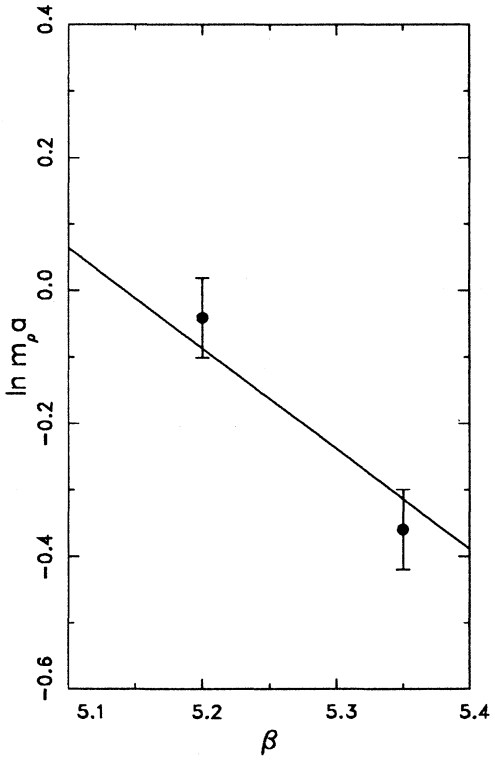

FIG. 7. The scaling behavior of the ρ mass extrapolated to zero quark mass and corrected for lattice artifacts. The solid line is the asymptotic scaling prediction for the slope.

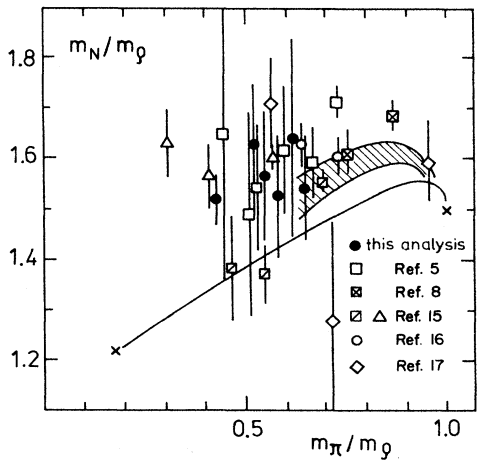

FIG. 8. The ratio m_N/m_ρ vs m_π/m_ρ (Edinburgh plot). Our data (●) are shown on the background of a recent compilation, Ref. 1. The shaded area represents the region of quenched data.

TABLE V. Comparison of the particle masses at $\beta=5.20$ and $am=0.050$ with results reported in Ref. 5 that are based on a hybrid algorithm.

	Hybrid method 16×8^3, Ref. 5	Pseudofermions 24×12^3
π	0.613±0.002	0.620±0.004
ρ	1.16 ±0.02	1.12 ±0.02
N	1.79 ±0.14	1.76 ±0.17
A_1	1.51 ±0.10	1.45 ±0.09
ϵ	1.08 ±0.04	1.06 ±0.03
ρ'	1.25 ±0.08	1.30 ±0.06
N'	2.06 ±0.40	2.09 ±0.14

consistent with a linear dependence on the quark mass, extrapolating to a vanishing value for massless quarks. This is shown in Fig. 9 and is consistent with the square-root dependence plotted in Figs. 6. (The pion data points in Figs. 6 do not fit a simple straight line.) While the 5.35 data fit a straight line through the origin quite well, the high mass 5.20 point lies slightly lower. We would expect that the slope of the curves would scale like the lattice spacing a. If we fit the 5.20 data with a straight line through the origin, the slopes of the 5.20 and 5.35 data are in the ratio 7.6/7.1—less than the value 1.25 from scaling, but in the right direction. It appears that for the pion the scaling law sets in at higher β values only. [This problem has been investigated in detail in quenched color SU(2) (Ref. 19) and also quenched SU(3) (Ref. 20).]

Fixing the lattice spacing from the ρ mass, we extracted the quark mass value from the slope $(m_\pi a)^2/(ma)$. By relating[21] the quark mass $m(a)$ with the renormalization-group-invariant mass defined in Ref. 22, we obtain

$$m_q^{\mathrm{RGI}}=\begin{cases}3.05m(a(5.20))=9.3\pm1.0\ \mathrm{MeV}\ ,\\ 3.09m(a(5.35))=7.3\pm1.0\ \mathrm{MeV}\ .\end{cases}$$

These numbers ($\overline{\mathrm{MS}}$ scheme) are consistent with the mean value of 10±3 MeV from current algebra and QCD sum rules.[22]

A nonzero value of the quark condensate

$$\langle\bar{q}q\rangle_{2\ \mathrm{flavors}}=\tfrac{1}{2}\sum_i\langle\bar{\chi}_i\chi_i\rangle$$

for vanishing quark mass signals the spontaneous breaking of chiral symmetry. This parameter is evaluated by taking the trace of the inverse Dirac operator

$$\langle\bar{q}q\rangle_{2\ \mathrm{flavors}}=\frac{1}{2V}\langle\mathrm{tr}(D+ma)^{-1}\rangle\ , \tag{9}$$

where V is the lattice volume. We calculated the diagonal elements of the inverse Dirac matrix as a byproduct of our pseudofermion inversion. Evaluating the same quantity during the computation of the quark propagators by means of the conjugate-gradient algorithm provides a consistency check on the pseudofermion method. Because of the limited number of source points within each configuration, the error bars in the latter case are somewhat bigger than in the former case. However, the mean values lie on top of each other. In addition we exploited the Ward identity

$$\langle\bar{q}q\rangle_{2\ \mathrm{flavors}}=\tfrac{1}{2}m\sum_{\mathbf{n},t}G_\pi(\mathbf{n},t)\ , \tag{10}$$

where G_π is the pion propagator. Even though this calculation of the condensate is based on the same matrix inversion, it involves all elements of a column of the propagator. Again, we see nice agreement between the methods. We show the measured values of the quark condensate in Fig. 10(a). Extrapolating these values

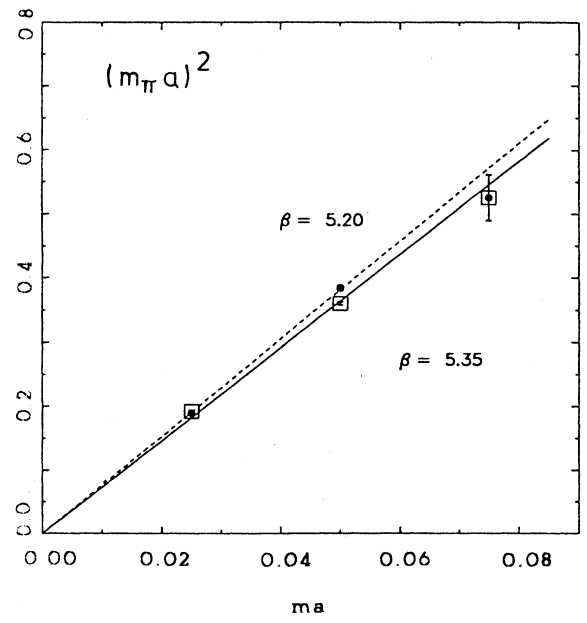

FIG. 9. Linear fits of $(m_\pi a)^2$ vs ma for $\beta=5.20$ (dashed line) and $\beta=5.35$ (solid line). The data points at 0.025 and 0.075 coincide for both β values. (The dashed line is a fit to the first two points only.)

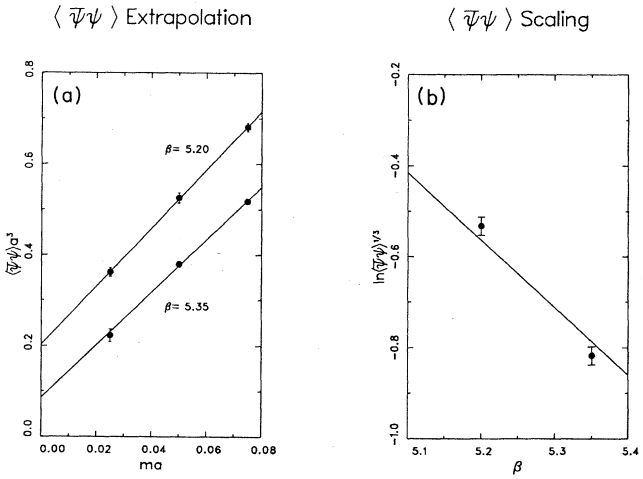

FIG. 10. (a) The mass dependence of the quark condensate at $\beta=5.20$ and 5.35. (b) The quark condensate extrapolated to zero quark mass; the solid line is the asymptotic scaling curve.

linearly down to a zero quark mass, we find a nonzero value for the condensate, consistent with the spontaneous breakdown of chiral symmetry. It is clear from Fig. 10(b) that these extrapolated data are close to the predicted slope from asymptotic scaling. In the same manner as before, we may thus extract the renormalization-group-invariant value of the quark condensate:

$$\langle \bar{q}q \rangle^{\mathrm{RGI}}_{1\ \mathrm{flavor}} = (208 \pm 22\ \mathrm{MeV})^3 ,$$

which is quite close to the current-algebra value of 190±20 MeV derived from Ref. 22.

Encouraged by this result, we exploit the current-algebra relation

$$f_\pi^2 = \frac{m}{m_\pi^2} \langle \bar{q}q \rangle_{2\ \mathrm{flavors}} \tag{11}$$

to calculate the leptonic pion decay constant. Inserting the numbers already determined, we find that

$$f_\pi = \begin{cases} 92 \pm 9\ \mathrm{MeV} & \text{for } \beta = 5.20 , \\ 86 \pm 9\ \mathrm{MeV} & \text{for } \beta = 5.35 , \end{cases}$$

which is in reasonable agreement with the experimental value of 93 MeV.

V. THE HEAVY-QUARK POTENTIAL

There is now compelling theoretical evidence that the potential between heavy static quarks in the pure gauge theory rises linearly with separation R (Ref. 23). Including light dynamical quarks in the theory should change this. Spontaneous quark pair creation in the stretched field between heavy separated quarks will screen the quark color charge at distances greater than about a fm. This turns the potential into one with a short range between the bound state of a heavy quark and a light antiquark and its charge conjugate. To investigate this, we have extracted the potential from the Wilson loops in a standard way:

$$V(R) = -\frac{1}{T} \ln W(R,T) \quad \text{for large } T ,$$

$$W(R,T) = \left\langle \frac{1}{3} \mathrm{tr} \prod_{\zeta} U \right\rangle \quad \text{for } R \times T \text{ loop } \zeta .$$

The logarithms of the Wilson loops are shown in Fig. 11 for $[\beta, ma] = [5.35, 0.025]$. Weakening, as usual, the "large-T" condition to $T \geq R$, a linear behavior fits the data remarkably well, down to the largest T extent for $R = 1, 2, 3$. For $R = 4$, the slope can be proved to be linear only down to $T = 10$, beyond that value the data is too noisy. At $R = 5$ and 6 only one or two points satisfy the condition $T \geq R$ before the data dips into noise, so we did not attempt to extract a value for the potential there.

In an unquenched calculation such as this, the potential depends on the quark mass. We approximate this dependence by a linear function to extrapolate Va to zero quark mass, as shown in Fig. 12 for $\beta = 5.35$. The mass dependence is slightly steeper for smaller β.

In order to calculate the potential in physical units we pursued two different strategies.

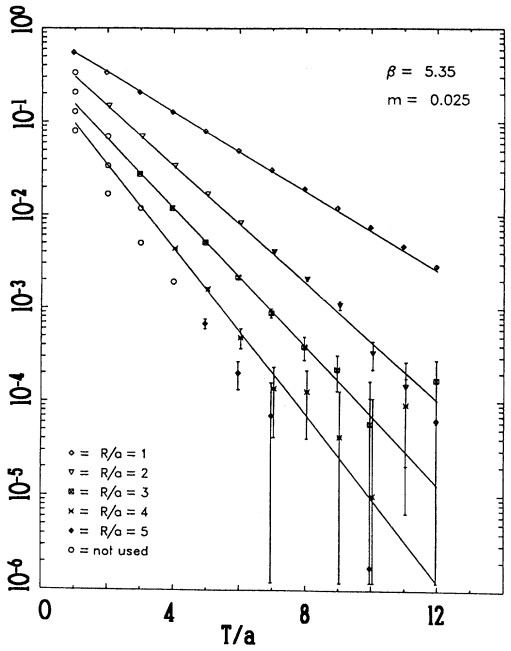

FIG. 11. The logarithms of Wilson loops $\ln W(R,T)$ as linear functions of T at $[\beta, ma] = [5.35, 0.025]$.

(i) We first fitted the zero-quark-mass potential by a Coulomb plus linear ansatz for both β values separately. The *ratio* of the two σa^2 values is then obtained as $(1.43)^2$, in agreement with the ratio resulting from the ρ masses. However, if we compare the *absolute scale* determined from the ρ mass measurement to that extracted from an unscreened form of the potential, we find $a^2(\mathrm{pot})/a^2(\rho) = 0.45 \pm 0.03$. Even though a deviation of this ratio from 1 cannot be ruled out as a consequence of

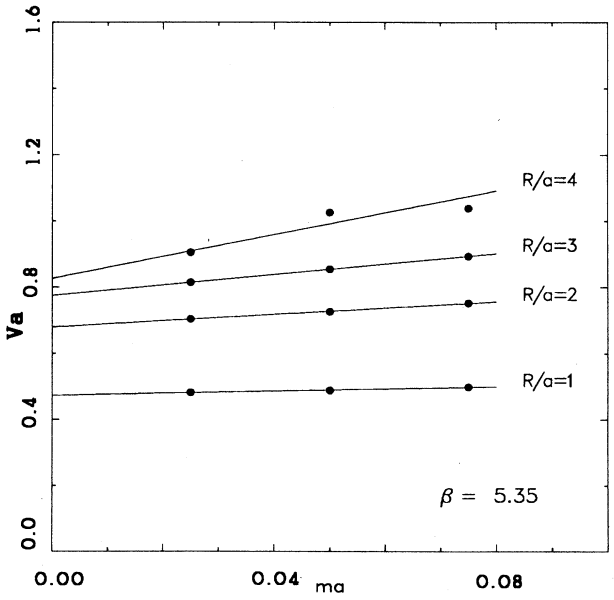

FIG. 12. The values of the interquark potential Va for distances $R = 1, \ldots, 4$ in lattice units at $\beta = 5.35$.

lattice artifacts, such a small value can be considered as very unlikely, and we reject this procedure as an inconsistent interpretation of the data.

(ii) Adopting instead the lattice spacing from the ρ mass measurement we find the potential in physical units (GeV vs fm) as shown in Fig. 13. While the two sets of data for the different β values have been mapped onto each other by using the measured ρ mass ratio in lattice units, the β-dependent heavy-quark self-energies are removed by adjusting one point of the potential. We parametrize the data in terms of a screening length μ^{-1}:

$$V(R)=\left[-\frac{\alpha}{R}+\sigma R\right]\frac{1-e^{-\mu R}}{\mu R}\ , \tag{12}$$

which has the correct Coulombic behavior at small distances and approaches a constant at large distances. We can think of the constant $\delta=\sigma/\mu$ as the splitting energy of the heavy-quark pair. If we choose to keep $\sigma=(400\ \text{MeV})^2$ fixed, then a fit returns $\alpha=0.21\pm0.01$; this is close to the value in the quenched case. We then also find the screening length

$$\mu^{-1}=0.9\pm0.2\ \text{fm}\ .$$

This scale lies in the range we expect.[2] The splitting energy is $\delta\approx800$ MeV, which is in reasonable agreement with what we would expect from quarkonium models. For comparison we show the world's average of quenched potential values, in which the strength of the Coulomb interaction is of $\alpha\approx0.26$ and the string tension is set to $\sqrt{\sigma}=400$ MeV. The deviation of the data from the unscreened form of the potential is evident in this picture and it indicates the breaking of the flux tube between the heavy static quarks.

It should be stressed again, however, that these conclusions depend on the fact that we measure the ρ mass in the same computer experiment in which we measure the potential. Had we not done this and let the scale vary freely, the data points could have migrated along the arrow onto the solid line in the figure. As discussed in the preceding paragraphs, the price to be paid would have been a value of the lattice spacing inconsistent with that from our simultaneous ρ mass measurement.

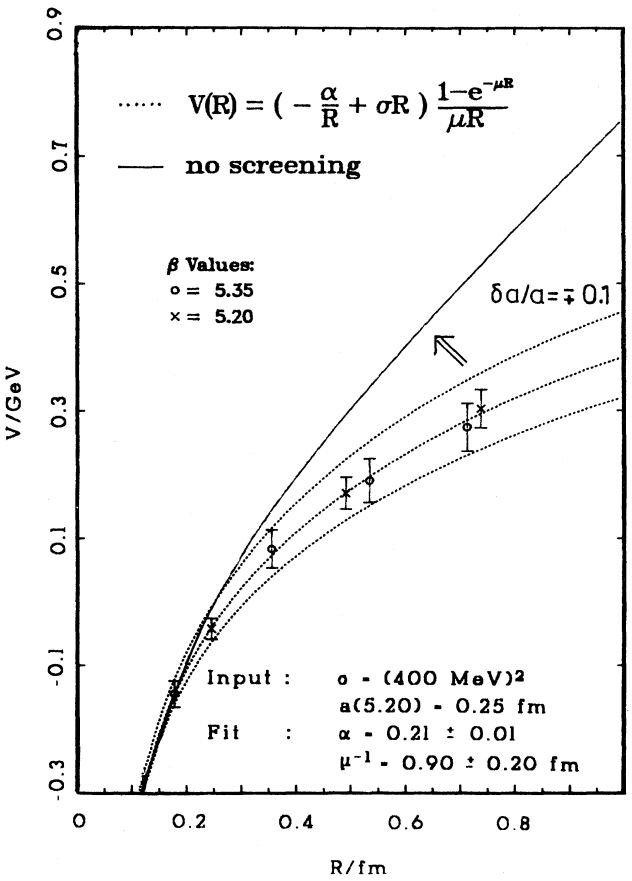

FIG. 13. The interquark potential in physical units as inferred from the ρ mass measurements. The dotted line through the data points describes the fit to a screened form of the potential (the neighboring dotted lines indicate the change of the potential if the lattice spacing a is altered by $\mp10\%$). The standard (unscreened) QCD potential is shown by the solid line for a string tension $\sigma=(400\ \text{MeV})^2$ and a fixed coefficient of the Coulomb term $\alpha=0.26$.

VI. SUMMARY

We have shown that lattice gauge theories with light quarks provide a reasonably consistent picture for some of the basic properties of the low-lying hadron states.

(1) While the pattern of hadron masses in the simulation is *qualitatively* as seen experimentally it is not yet *quantitatively* satisfactory. The pion-to-ρ as well as the nucleon-to-ρ mass ratios are expected to be smaller. Additional data—especially at lower quark masses—are needed to test this aspect of the theory.

(2) There is a clear indication for spontaneous breaking of chiral symmetry. Our data are consistent with a pion mass which extrapolates to zero for zero quark mass, associated with a finite quark condensate. Physical quantities such as the renormalization-group-invariant quark mass and the quark condensate match current-algebra values. The pion decay constant comes out numerically correct.

(3) At large distances, we have found indications for a breaking of the color flux tubes between heavy static quarks. This is expected from the spontaneous creation of quark pairs in the color force field. In order to deduce this, we have to rely on our simultaneous measurements of the ρ mass and the potential so that we can fix the lattice spacing.

Our analysis is not disrupted by finite-size effects or by systematic errors. We have demonstrated this by extensive internal consistency checks, by comparison to SU(2) and particularly by comparisons with Ref. 5, which is work based on a hybrid method applied to a $(2\cdot16)\times8^3$ lattice. Thus, even in view of the first point mentioned above—which is, of course, a critical one—we find reasonable physics emerging from this size lattice. Improvements are expected from ongoing computations at quark masses of $ma=0.010$ and smaller.

ACKNOWLEDGMENTS

This analysis has mainly been carried out at the Minnesota Supercomputer Center; additional computer time had been available at HLRZ/Kernforschungsanlage Jülich. This research was supported in part by DOE Grant No. DE-AC-0240105, grants of the Minnesota Supercomputer Institute, the Minnesota Supercomputer Center Inc., the Deutsche Forschungsgemeinschaft and the West German Bundesministerium für Forschung und Technologie.

[1]See, e.g., M. Fukugita, in *Field Theory on the Lattice,* proceedings of the International Symposium, Seillac, France, 1987, edited by A. Billoire *et al.* [Nucl. Phys. B, Proc. Suppl. **4**, 105 (1988)].

[2]E. Laermann, F. Langhammer, I. Schmitt, and P. M. Zerwas, Phys. Lett. B **173**, 437 (1986); **173**, 443 (1986).

[3]F. Fucito, E. Marinari, G. Parisi, and C. Rebbi, Nucl. Phys. **B180** [FS2], 369 (1981).

[4]E. V. E. Kovacs, D. K. Sinclair, and J. B. Kogut, Phys. Rev. Lett. **58**, 751 (1987); for $N_T=4$ data see Fukugita's compilation, in *Field Theory on the Lattice* (Ref. 1).

[5]M. P. Grady, D. K. Sinclair, and J. B. Kogut, Phys. Lett. B **200**, 149 (1988).

[6]G. Bhanot, U. Heller, and I. O. Stamatescu, Phys. Lett. **129B**, 440 (1983).

[7]J. Potvin, in The 1988 International Symposium on Lattice Gauge Theory, Fermilab, 1988 (unpublished).

[8]M. Campostrini, K. Moriarty, J. Potvin, and C. Rebbi, Phys. Lett. B **193**, 78 (1987); J. Potvin *et al.*, in *Field Theory on the Lattice* (Ref. 1), p. 140.

[9]A. D. Kennedy, J. Kuti, S. Meyer, and P. J. Pendleton, Phys. Rev. Lett. **54**, 87 (1985).

[10]H. Kluberg-Stern, A. Morel, O. Napoly, and B. Peterson, Nucl. Phys. **B220** [FS8], 447 (1983); J. B. Kogut, M. Stone, H. W. Wyld, S. H. Shenker, J. Shigemitsu, and D. K. Sinclair, *ibid.* **B225** [FS9], 326 (1983).

[11]K. D. Born, E. Laermann, F. Langhammer, T. F. Walsh, and P. M. Zerwas, following paper, Phys. Rev. D **10**, 1664 (1989).

[12]A. Hasenfratz and P. Hasenfratz, Phys. Lett. **104B**, 489 (1981); H. S. Sharatchandra, H. J. Thun, and P. Weisz, Nucl. Phys. **B192**, 205 (1981).

[13]W. J. Stirling, in *Lepton and Photon Interactions,* proceedings of the International Symposium on Lepton and Photon Interactions at High Energies, Hamburg, West Germany, 1987, edited by W. Bartel and R. Rückl [Nucl. Phys. B, Proc. Suppl. **3**, 715 (1988)].

[14]Note that a change of the lattice spacing $\Lambda_{\overline{\rm MS}}$ by a factor of 3 alters the value of the quark condensate by a factor of 27.

[15]S. Gottlieb, W. Liu, D. Toussaint, R. Renken, and R. L. Sugar, Phys. Rev. Lett. **59**, 1513 (1987); S. Gottlieb *et al.*, in *Field Theory on the Lattice* (Ref. 1), p. 155.

[16]M. Fukugita, S. Ohta, Y. Oyanagi, and A. Ukawa, Phys. Lett. B **191**, 164 (1987).

[17]M. Fukugita, Y. Oyanagi, and A. Ukawa, Phys. Lett. B **203**, 145 (1988).

[18]D. Toussaint, in The 1988 International Symposium on Lattice Gauge Theory, Fermilab, 1988 (unpublished).

[19]A. Billoire, R. Lacaze, E. Marinari, and A. Morel, Nucl. Phys. **B251** [FS13], 581 (1985), and work referred to there.

[20]K. C. Bowler, R. D. Kenway, D. Roweth, and D. B. Stephenson, Nucl. Phys. **B301**, 304 (1988).

[21]M. Göckeler, Phys. Lett. **142B**, 197 (1984).

[22]J. Gasser and H. Leutwyler, Phys. Rep. **87**, 77 (1982).

[23]P. Hasenfratz, in *Proceedings of the XXIII International Conference on High Energy Physics,* Berkeley, California, 1986, edited by S. C. Loken (World Scientific, Singapore, 1987).